PHYSICAL REVIEW B **86**, 041404(R) (2012)

Engineering gratings for light trapping in photovoltaics: The supercell concept

Emiliano R. Martins,[1,*] Juntao Li,[2,1,†] YiKun Liu,[2,1] Jianying Zhou,[2] and Thomas F. Krauss[1]
[1]*School of Physics and Astronomy, University of St Andrews, St Andrews, Fife KY16 9SS, UK*
[2]*State Key Laboratory of Optoelectronic Materials and Technologies, Sun Yat-sen University, Guangzhou, 510275, China*
(Received 16 January 2012; published 9 July 2012)

The question of the optimal surface structure for light trapping is widely debated in thin-film solar cell research. Here we propose a generic design approach that can tailor the strength of the diffraction orders of a periodic structure. Our approach is based on a supercell geometry that is able to suppress the low orders that do not couple into the quasiguided modes of the thin film. We demonstrate the concept theoretically and experimentally, showing that the supercell outperforms conventional gratings.

DOI: 10.1103/PhysRevB.86.041404 PACS number(s): 78.67.Pt, 88.40.hj, 42.25.Fx, 42.30.Kq

Thin-film technology can dramatically reduce the cost of solar cells. A central aspect of this technology is the employment of light-trapping structures to compensate for the otherwise poor absorption in the thin film, especially in the case of indirect bandgap materials such as crystalline and microcrystalline silicon. Light trapping is hence achieved by the excitation of quasiguided modes or resonances in the absorbing thin film and is facilitated by metallic[1,2] or dielectric[3–6] nanostructures. Such nanostructures occur either in the form of random surface roughness, which excites a large number of diffraction orders or Fourier components, or alternatively in the form of ordered gratings, which excite only a well-defined Fourier spectrum. We speculate that the optimum light-trapping structure lies somewhere between these two extremes; while the Fourier components generated by random scattering are too weak, there are not enough of them created by regular ordered gratings. Furthermore, neither extreme provides sufficient degrees of freedom to account for the wavelength-dependent absorption of indirect bandgap active materials such as silicon. While a number of authors have already addressed this issue using numerical optimization methods,[7–10] we are not aware of any *ab initio* design that provides a suitable solution.

Here we propose a novel grating design approach that opens up a broader parameter-space while maintaining control over the diffracted orders. The proposed concept is a general way of controlling light based on the tailoring of the Fourier components of periodic structures. Even though we focus on the light-trapping application, this concept increases the degrees of freedom of light control in general. Therefore, the idea can be explored in a broad range of applications such as cavity Q-factor control of distributed feedback lasers or tailor of light emission from light-emitting devices (LEDs). Our design is based on the idea of a supercell, i.e., a larger period grating with a unit cell containing a fine structure. The purpose of the large period grating is to provide many Fourier components, while the fine structure is used to control their amplitude. The concept is illustrated in Fig. 1, where we show a scanning electron microscope (SEM) micrograph of such a supercell grating fabricated in our laboratory, and a sketch of its operating principle, which is based on suppressing diffraction orders that do not couple into quasiguided modes of the thin film. We show theoretically that our novel design outperforms standard grating designs and confirm the operation of a supercell grating experimentally. Even though the concept is illustrated assuming crystalline silicon solar cells, it can be readily extended to other types of absorbing materials.

The reasoning behind our design approach is as follows. A random texture can be understood as having an infinite number of diffraction orders. For this reason, when random structures are used for light trapping, the absorption enhancement is broadband and independent of the incidence angle. In contrast, periodic structures have fewer diffraction orders that can couple to a finite number of quasiguided modes. Because the light is strongly scattered into only a few diffraction angles, the absorption is very strongly enhanced around the resonant wavelengths, yet the enhancement is negligible otherwise. Also, the smaller the period of the grating, the fewer useful diffraction orders there are. From these considerations, we propose that the best grating design lies between these two domains; i.e., it requires broadband operation, with many diffraction orders, yet it also requires strong absorption enhancement into each excited resonance. Naively, this requirement could be met by a periodic structure with a large period. In fact, in the limit, a random structure can be understood as a periodic structure with infinite period. However, simple modelling shows that large period gratings do not perform better than wavelength-scale gratings, as we highlight in Fig. 2, where we compare the resonances excited in a thin-film slab by a wavelength-scale optimized grating [$a = 400$ nm; Fig. 2(a)], a large period grating [$a = 1800$ nm; Fig. 2(b)], and a supercell grating [$a = 1800$ nm; Fig. 2(c)]. The results for unpolarized light and all angles of incidence can be found in Fig. 4. The large period grating excites a large number of resonances, yet these are relatively weak; the wavelength-scale grating excites fewer, yet stronger resonances, while the supercell excites many and strong resonances. The poor performance of the large period grating [Fig. 2(b)] is therefore due to diffraction losses, i.e., the excitation of low diffraction orders with a diffraction angle that is smaller than the total internal reflection angle of the absorbing slab; these orders perform only a single pass through the absorbing material and cannot excite quasiguided modes, so are only weakly absorbed. According to standard diffraction theory, the lowest diffraction orders are the strongest ones; hence the high orders that do couple into quasiguided modes tend to be weaker; this explains the decrease of the resonance strength between the small ($a =$ 400 nm) period and large ($a = 1800$ nm) period gratings.

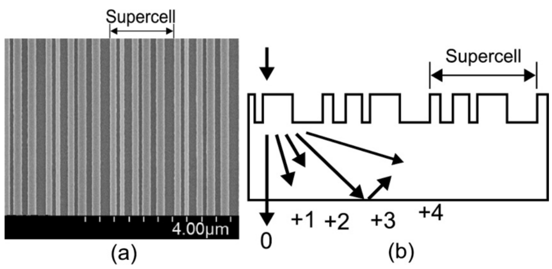

FIG. 1. Supercell grating. (a) SEM micrograph of the supercell grating used in the experiments. (b) Sketch of the operating principle. The diffraction orders that are not able to couple into quasiguided modes of the thin film (here: +1, +2) are suppressed, while the diffraction orders that do couple into such modes (here: +3, +4) are enhanced.

We used a 400 nm thin film for the comparison because this thickness is sufficient to support multiple modes in the wavelength regime of interest, yet it is thin enough for the absorption of unguided (single-pass) light to be weak, thus allowing us to highlight the benefit of coupling into quasiguided modes. A numerical parameter scan for the $a = 400$ nm wavelength-scale grating yielded an optimum groove depth of 100 nm and a fill factor of 50%; these two parameters were then adopted for the other types of gratings as well. The calculations were performed using the Rigorous Coupled Wave Analysis (RCWA).[11] Our model already reaches convergence for 50 plane waves, and this is the truncation value used for all reported simulations. Also, the RCWA results were compared to finite-element results and excellent agreement was observed. The incident light is perpendicular to the grating, and the polarization is TE (electric field parallel to the groove lines). For simplicity and clarity, no antireflection (AR) coatings were assumed. The integrated absorption is calculated in the standard way[12] by integrating the entire spectrum between 300 and 1200 nm wavelength and approximating the solar photon density as black-body

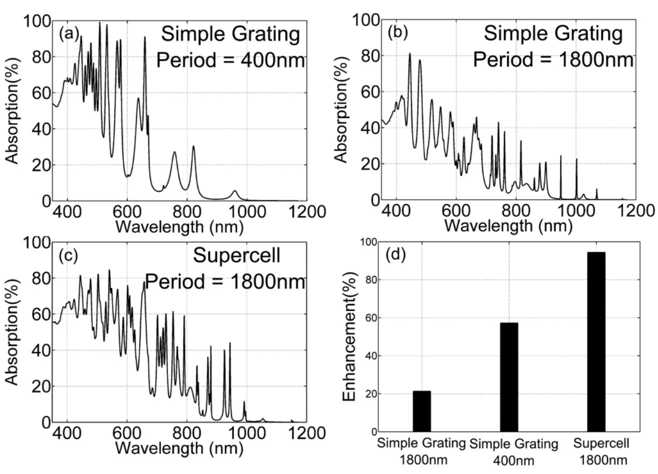

FIG. 2. Comparison between the absorption spectrum of a 400 nm slab of silicon for TE polarization (electric field parallel to the grating lines) and perpendicular incidence. (a) Optimized simple grating. (b) Large period simple grating. (c) Large period supercell. (d) Integrated absorption enhancement compared to an unpatterned slab of the same thickness.

radiation at 5800 K.[12] The integrated absorption enhancement compared to an unpatterned slab is shown in Fig. 2(d). A large period grating ($a = 1800$ nm) shows 21% higher absorption than the slab, the optimized wavelength-scale grating ($a = 400$ nm) shows 57% enhancement, while the supercell ($a = 1800$ nm) shows the highest enhancement at 94%.

The supercell grating achieves this high enhancement because it has lower diffraction losses. We reduce the diffraction losses by engineering the unit cell of the large period grating with the aim of shifting the diffraction energy from lower to higher orders. This is realized by tailoring the Fourier spectrum of the grating. This process is illustrated in Fig. 3 and is based on the well-known property of the Fourier series that a spatial shift of the function induces a phase shift of the Fourier series, as shown in Eq. (1):[13]

$$f(x - x_0) = F(m)\exp\left(-i\frac{2\pi}{a}mx_0\right), \tag{1}$$

where $F(m)$ is the Fourier series of $f(x)$, m is an integer corresponding to the diffraction order, a is the period, and x_0 is the spatial translation. Since the phase shift depends on x_0 and on m, the spatial shift can be chosen to provide destructive interference for lower orders and constructive interference for higher orders. In this example, we aim to couple light mainly in the wavelength region above 600 nm, because this is the spectral region where the absorption in silicon is very low.[12] Once the wavelength region of interest is defined, the highest diffractive order is given by the ratio between the period and the wavelength. In this example, the period is 1800 nm, which gives a ratio of 3; i.e., the $m = 3$ order couples into air for $\lambda < 600$ nm, and into the slab for $\lambda > 600$ nm, while orders 1 and 2 always diffract into air and must therefore be suppressed.

The next step of the design is to superimpose multiple gratings in order to reduce orders 1 and 2. The selection of the required spatial shifts is done using a simple binary search. In the binary search, an array of pixels is defined. Pixels defined as 1 represent ridges and pixels defined as 0 represent grooves. The pixel size is arbitrary, and in our example, we choose fabrication limitations as the constraint criteria, i.e., 112 nm. Therefore, there are 32 pixels for the chosen period of 1800 nm, with a minimum block size of 2 pixels.

A binary search is performed by swapping the value of each pixel and calculating the Fourier transform of the total pixel array each time a pixel is changed. The resulting supercell consists of 10 blocks, with the following sequence of number of pixels: **4**, 2, **3**, 4, **2**, 2, **3**, 5, **4**, 3. This sequence, with bold representing ridges, is also shown schematically in Fig. 3.

Figure 4(a) shows the resulting diffraction efficiency of the supercell grating for each diffraction order. The diffraction efficiency is calculated with the RCWA and corresponds to the amount of energy diffracted into each order inside the high index material. Please note that the RCWA method takes multiple scattering fully into account, so is not restricted to weak perturbations. In order to facilitate the comparison between the different orders, the diffraction efficiency is normalized to the highest value occurring in the dataset. As a result of the suppression of orders 1 and 2, the diffraction efficiencies of these orders are strongly reduced. For example, at 600 nm, the diffraction efficiency of the first order is less than

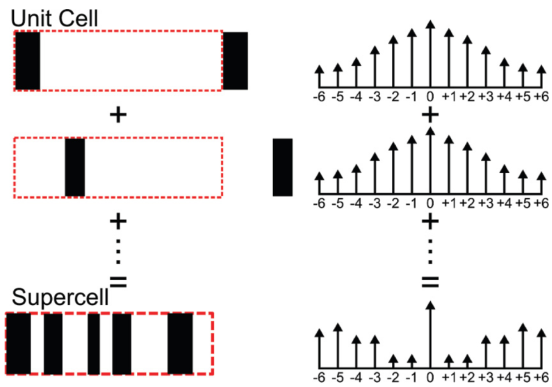

FIG. 3. (Color online) Design principle of the supercell grating. The supercell consists of a superposition of multiple low filling factor gratings with the same period. The gratings are spatially offset from one another, which imposes a phase shift between the diffraction orders. This phase shift is used to design destructive interference for the lower orders and constructive interference for the higher orders. Here we suppress the ±1, ±2 diffractive orders and enhance the higher orders.

10% of the sixth order. It is quite remarkable that, even with high dielectric contrast and deep grooves, the desired effect of suppressing the first two orders, as suggested by our simple picture (Fig. 3), is clearly seen in the corresponding diffraction efficiencies. The diffraction efficiency of the zero order is very similar to that of the simple grating, and its magnitude reaches a minimum around 550 nm wavelength.

The benefit of the supercell approach on solar cell operation is best shown by calculating the integrated absorption over all possible input angles. Figures 4(b)–4(d) show a wavelength-integrated polar plot to highlight the angular dependence, and it is clear that the supercell provides the highest performance at almost all angles, especially for the (most relevant) unpolarized case [Fig. 4(d)].

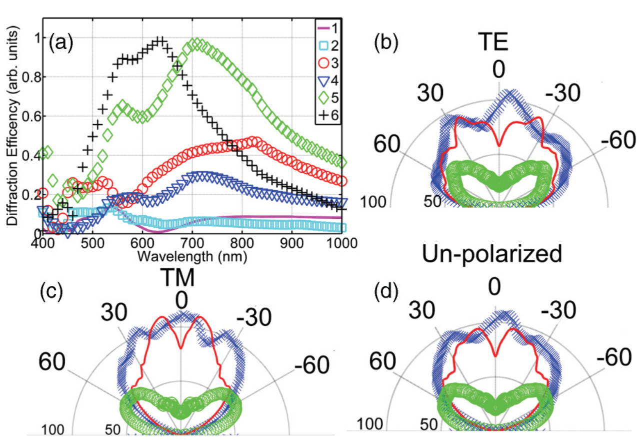

FIG. 4. (Color online) (a) Diffraction efficiency of the supercell in transmission. Modes 1 and 2 (solid line and squares) are not able to couple to quasiguided modes and have therefore been suppressed. It is evident that the suppression favours the modes that do couple to quasiguided modes (No. 3–6) and that the method is effective over a large wavelength range. (b)–(d) Comparison between the performances of a wavelength-scale optimized conventional grating (period a = 400 nm, red solid line), a large period grating (a = 1800 nm, green circles) and the supercell grating (a = 1800 nm, blue crosses) over multiple angles of incidence. Even though the majority of research in the field is concerned with wavelength-scale gratings, we show that a large period grating engineered to suppress unwanted diffraction orders provides better performance.

Finally, we verify the concept experimentally by fabricating a supercell grating and comparing its performance with the model. We employ electron beam lithography to fabricate the grating of Fig. 1(a) on a silicon on insulator (SOI) wafer. The available SOI consists of a 220 nm silicon device layer on top of a 2 μm silicon dioxide layer, supported by the handle wafer. Even though the substrate prevents us from measuring the absorption on the thin-film directly, the oxide layer ensures that the 220 nm silicon layer acts as a waveguide and allows all properties of quasiguided mode excitations to be seen. It is well known that the excitation of a quasiguided mode is manifested as a resonance in the reflectance spectrum.[14] For this reason, we use an integrating sphere to collect the reflected light from the SOI and thus probe the quasiguided mode resonances. Because the transmitted light is absorbed by the substrate, the reflectance is also a measurement of the total absorption of the SOI, as $A = 1 - R$.

Figure 5 shows a comparison between experiment and RCWA model. Note that no fitting parameters have been used; also, the simulation is performed using the supercell parameters as designed and no adjustment of the model to the measured values of the fabricated supercell was made. In this way, the excellent agreement between measurement and theory also shows how robust the supercell is to fabrication imperfections. It is clear that a number of resonances (e.g., at 770, 830, and 900 nm) are being excited that are closely matched by the simulation. Since we use a different slab thickness than in Fig. 2, the spectral position of the resonances cannot be directly compared to those shown here. Overall, the excellent agreement demonstrated in Fig. 5 verifies our RCWA calculations and thus confirms the potential of the supercell concept for solar cell applications.

Since the vast majority of the literature reports enhancements obtained for perpendicular incidence, we also use normal incidence values for comparison. In this case, our optimized simple grating enhances the integrated absorption by 68.5% whereas the supercell provides an enhancement

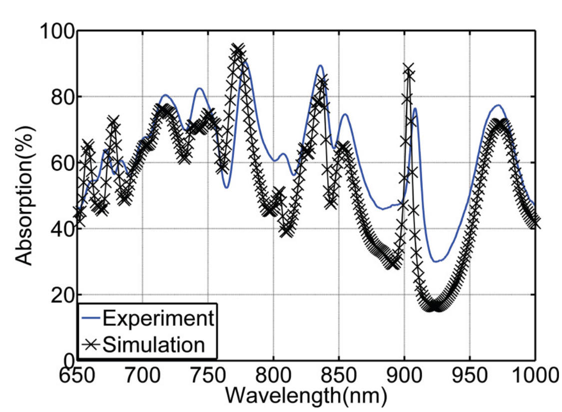

FIG. 5. (Color online) Absorption measurements of an SOI wafer patterned with a supercell grating. The agreement between measurement (blue solid curve) and RCWA simulation (black crosses) is quite remarkable given that there are no fitting parameters.

of 100%. Other contributions comparing the performance of simple with complex gratings usually explore the third dimension, which makes fabrication much more challenging. For example, an efficient 3D design has been proposed that can enhance the absorption by 110% in 400 nm thick silicon solar cells,[9] a performance comparable to the one achieved by our 1D supercell. It has also been shown that a complex structure combining a front binary grating with a triangular back grating can reach up to 97.2%.[15] In a thorough study, it was shown that a simple 2D binary grating in the presence of AR coatings can increase the absorption by 55% compared to an AR-coated bare substrate.[16]

We highlight that the result shown here only serves as a proof-of-concept example and that we have not conducted an exhausting parameter scan. We are therefore confident that even higher efficiencies can be achieved by following our recipe of shifting the energy from lower to higher diffraction orders. Importantly, the smallest feature size of the example supercell investigated here is 112 nm, which is compatible with large scale production using nano-imprint lithography. Therefore, the supercell design concept we introduce here may be able to provide the ideal optical structure capable of approaching the theoretical light trapping limit[4,16–19] while also being technologically feasible.

This work was funded by the Scottish Universities Physics Alliance (SUPA), the Chinese agencies National Key Basic Research Special Foundation (G2010CB923204), Chinese National Natural Science Foundation (10934011), and “985 project” of Sun Yat-sen University.

[*]erm43@st-andrews.ac.uk
[†]lijt3@mail.sysu.edu.cn

[1]H. A. Atwater and A. Polman, Nat. Mat. **9**, 205 (2010).
[2]L. Novotny, Phys. Rev. Lett. **98**, 266802 (2007).
[3]P. Bremel, C. Luo, L. Zeng, L. C. Kimerling, and J. D. Joannopoulos, Opt. Express **15**, 16986 (2007).
[4]Z. Yu, A. Raman, and S. Fan, Proc. Natl. Acad. Sci. USA **107**, 17491 (2010).
[5]C. Battaglia, J. Escaree, K. Soderstrom, M. Charriere, M. Despeisse, F.-J. Huag, and C. Ballif, Nat. Photonics **5**, 535 (2011).
[6]A. Abass, K. Q. Le, A. Alu, M. Burgelman, and B. Maes, Phys. Rev. B **85**, 115449 (2012).
[7]S. Fahr, C. Rockstuhl, and F. Lederer, Appl. Phys. Lett. **92**, 171114 (2008).
[8]A. Lin and J. Phillips, Sol. Energy Mater. Sol. Cells **92**, 1689 (2008).
[9]S. B. Mallick, M. Agrawal, and P. Peumans, Opt. Express **18**, 5691 (2010).
[10]X. Sheng, S. G. Johnson, J. Michel, and L. C. Kimerling, Opt. Express **19**, A841 (2011).
[11]M. G. Moharam, D. A. Pommet, E. B. Grann, and T. K. Gaylord, J. Opt. Soc. Am. A **12**, 1077 (1995).
[12]S. M. Sze, *Physics of Semiconductor Devices* (John Wiley & Sons, New York, 1981).
[13]R. N. Bracewell, *The Fourier Transform and Its Application* (McGraw-Hill, New York, 1983).
[14]S. Fan and J. D. Joannopoulos, Phys. Rev. B **65**, 235112 (2002).
[15]J. G. Mutitu, S. Shi, C. Chen, T. Creazzo, A. Barnett, C. Honsberg, and D. Prather, Opt. Express **16**, 15238 (2008).
[16]A. Bozzola, M. Liscidini, and L. Andreani, Opt. Express **20**, A224 (2012).
[17]Z. Yu, A. Raman, and S. Fan, Opt. Express **18**, A366 (2010).
[18]E. Yablonovitch and C. G., IEEE. Trans. Electron Devices **29**, 300 (1982).
[19]P. Campbell and M. A. Green, J. Appl. Phys. **62**, 243 (1987).